

Development of a CRISPR/Cas9-based therapy for Hutchinson–Gilford progeria syndrome

Olaya Santiago-Fernández¹, Fernando G. Osorio¹, Víctor Quesada^{1,2}, Francisco Rodríguez¹, Sammy Basso¹, Daniel Maeso¹, Loïc Rolas³, Anna Barkaway³, Sussan Nourshargh³, Alicia R. Folgueras¹, José M. P. Freije^{1,2*} and Carlos López-Otín^{1,2*}

CRISPR/Cas9-based therapies hold considerable promise for the treatment of genetic diseases. Among these, Hutchinson–Gilford progeria syndrome, caused by a point mutation in the *LMNA* gene, stands out as a potential candidate. Here, we explore the efficacy of a CRISPR/Cas9-based approach that reverts several alterations in Hutchinson–Gilford progeria syndrome cells and mice by introducing frameshift mutations in the *LMNA* gene.

Hutchinson–Gilford progeria syndrome (HGPS) is a rare disease characterized by aging-like manifestations emerging in childhood¹. Most cases (80–90%) result from a de novo point mutation in the *LMNA* gene—encoding the nuclear lamins A and C—which activates a cryptic splice site in exon 11 (c.1824C>T; p.Gly608Gly)^{2,3}. This event leads to the expression of progerin, a truncated lamin A variant with an internal deletion of 50 amino acids, which remains farnesylated, inducing morphological and functional alterations of the nuclear envelope⁴. A mouse model—*Lmna*^{G609G/G609G}—recapitulating the mutation and many of the clinical features of these children⁵, confirmed that HGPS is caused by progerin accumulation and not by the loss of normal lamin A^{5,6}. Several approaches against this syndrome were tested in preclinical models⁷, including farnesyltransferase inhibitors, which provided clinical benefits to HGPS patients^{8,9}.

CRISPR/Cas9 gene-editing tools constitute promising alternatives for diseases such as Duchenne muscular dystrophy¹⁰, metabo-
lopathies¹¹ and deafness¹². This system involves a Cas9 endonuclease directed by a single-guide RNA (sgRNA) that recognizes its target region, plus a protospacer-adjacent motif (PAM). The nuclease generates double-strand breaks in the DNA, repair of which through non-homologous end-joining produces insertions and deletions (indels)¹³. The finding that mosaic mice with both normal and prelamin A-producing progeroid cells have a completely normal phenotype¹⁴ indicates that a partial reduction in the accumulation of farnesylated lamin A products could be sufficient for an important phenotype relief.

On this basis, we developed a CRISPR/Cas9-based strategy against HGPS aimed at blocking the accumulation of lamin A and progerin. The *LMNA* gene encodes lamin C (exons 1–10) and lamin A (exons 1–12) through alternative splicing and polyadenylation. Since lamin A appears to be dispensable^{5,6}, our strategy would disrupt the last part of the *LMNA* gene, impeding lamin A/progerin production without affecting lamin C. We first designed an sgRNA (sgRNA-LCS1) with the 5'-NGG PAM sequence of *Streptococcus pyogenes* Cas9 to target *LMNA* exon 11 upstream of the HGPS mutation, in a region conserved across both humans and mice (Fig. 1a).

To test the efficacy of this approach, we cloned sgRNA-LCS1 or sgRNA-control in a lentiviral vector containing *S. pyogenes* Cas9 (lentiCRISPRv2) and used these to transduce *Lmna*^{+/+} and *Lmna*^{G609G/G609G} murine fibroblasts. As a result, indels of variable length were produced in sgRNA-LCS1-transduced cells, as assessed by capillary electrophoresis-based fragment analysis (Extended Data Fig. 1). Immunoblot analysis showed a significant decrease in the accumulation of progerin and lamin A, while lamin C levels were not affected (Fig. 1b). Likewise, immunofluorescence analysis demonstrated that numbers of progerin-positive nuclei were reduced by 74% in sgRNA-LCS1-transduced cells compared to sgRNA-control-transduced cells (Fig. 1c). Accordingly, we found a 65% decrease in the number of nuclear alterations in *Lmna*^{G609G/G609G} cells transduced with sgRNA-LCS1 compared to sgRNA-control-transduced cells (Fig. 1c).

To test this system in human cells, we infected *LMNA*^{G608G/+} fibroblasts from HGPS patients and *LMNA*^{+/+} fibroblasts with these lentiviral vectors. Similar to mouse fibroblasts, we observed different indels in the DNA (Extended Data Fig. 2), a decrease in progerin and lamin A by immunoblot (Fig. 1d), an 83% decrease in progerin-positive nuclei and a 39% reduction in the number of aberrant nuclei in sgRNA-LCS1- versus sgRNA-control-transduced HGPS cells (Fig. 1e).

We next tested, in vivo, this editing approach using *Lmna*^{G609G/G609G} mice as an HGPS animal model. We chose an adeno-associated virus 9 (AAV9) delivery vector due to its safety and broad tissue tropism. Given the packaging limit of these viruses (approximately 5 kb), we used *Staphylococcus aureus* Cas9 nuclease¹⁵ and designed a new sgRNA against the same region in exon 11 with the 5'-NNGRRT PAM sequence (sgRNA-LCS2). After packaging the vectors, with either sgRNA-LCS2 or the sgRNA-control, we injected intraperitoneally 2×10^{11} AAV9 genome copies in P3 *Lmna*^{G609G/G609G} mice (Fig. 2a). To assess editing efficiency, we performed Illumina sequencing of the target region in DNA from AAV9 target organs—liver, heart, muscle and lung—of injected mice. Notably, *Lmna* contained indels in $13.6 \pm 2.6\%$ of the genome copies in liver, $5.3 \pm 1.0\%$ in heart, $4.1 \pm 0.6\%$ in muscle and $1.1 \pm 0.2\%$ in lung (Fig. 2b,c; Extended Data Fig. 3; Supplementary Tables 1–4). Given the modest fraction of cells edited in vivo, the global decrease in progerin messenger (RNA) was too low for reliable detection by quantitative reverse transcription polymerase chain reaction (RT-qPCR) (Extended Data Fig. 4). However, immunohistochemical analysis revealed a significant reduction in progerin-positive nuclei in liver, heart and skeletal muscle from sgRNA-LCS2-transduced mice

¹Departamento de Bioquímica y Biología Molecular, Facultad de Medicina, Instituto Universitario de Oncología del Principado de Asturias, Universidad de Oviedo, Oviedo, Spain. ²Centro de Investigación Biomédica en Red de Cáncer, Madrid, Spain. ³William Harvey Research Institute, Barts and The London School of Medicine and Dentistry, Queen Mary University of London, London, UK. *e-mail: jmpf@uniovi.es; clo@uniovi.es

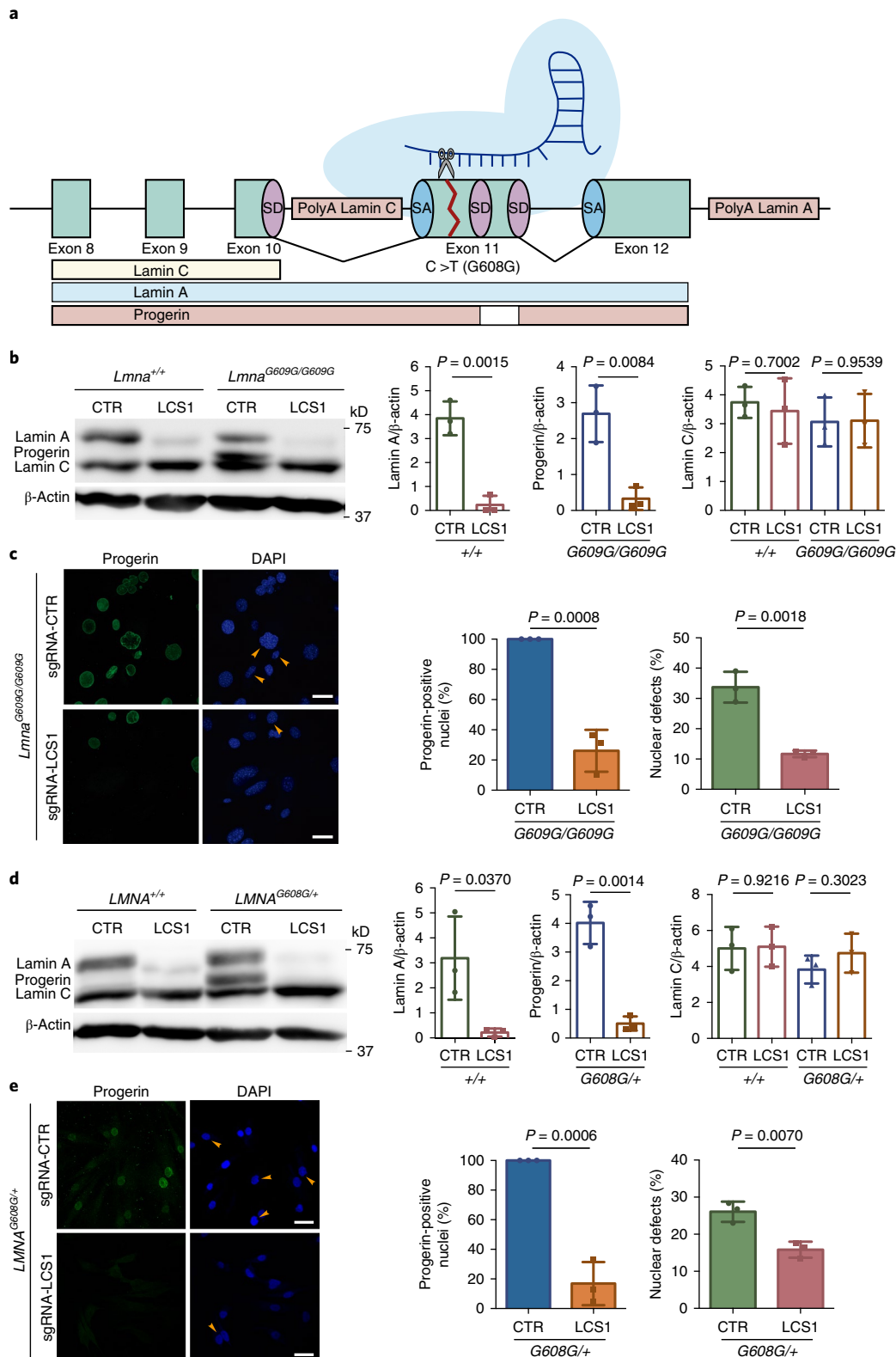


Fig. 1 | CRISPR/Cas9 testing in HGPS cellular models. a, sgRNA-LCS1 directs Cas9 nuclease against exon 11 of *LMNA* gene upstream of the HGPS mutation, disrupting lamin A and progerin without altering lamin C. **b**, Cropped immunoblot of lamin A, progerin and lamin C from WT and *Lmna*^{G609G/G609G} mouse embryonic fibroblasts (MEFs) transduced with sgRNA-control or sgRNA-LCS1 ($n = 3$ independent infections and MEF lines; two-tailed Student's *t*-test). **c**, Immunofluorescence analysis of progerin-positive nuclei and quantification of nuclear alterations by 4',6-diamidino-2-phenylindole (DAPI) staining ($n = 3$ independent infections and MEF lines; two-tailed Student's *t*-test). Arrowheads indicate nuclear aberrations of lamin A, progerin and lamin C from WT and *LMNA*^{G608G/+} human fibroblasts transduced with sgRNA-control or sgRNA-LCS1 ($n = 3$ independent infections; two-tailed Student's *t*-test). **d**, Cropped immunoblot of lamin A, progerin and lamin C from WT and *LMNA*^{G608G/+} human fibroblasts transduced with sgRNA-control or sgRNA-LCS1 ($n = 3$ independent infections; two-tailed Student's *t*-test). **e**, Progerin immunofluorescence and analysis of nuclear aberrations by DAPI staining ($n = 3$ independent infections; two-tailed Student's *t*-test). Arrowheads indicate blebbings and invaginations. Bar plots represent mean \pm s.d. and individual values are overlaid. Scale bars, 40 μ m. Uncropped blots are available as Source data.

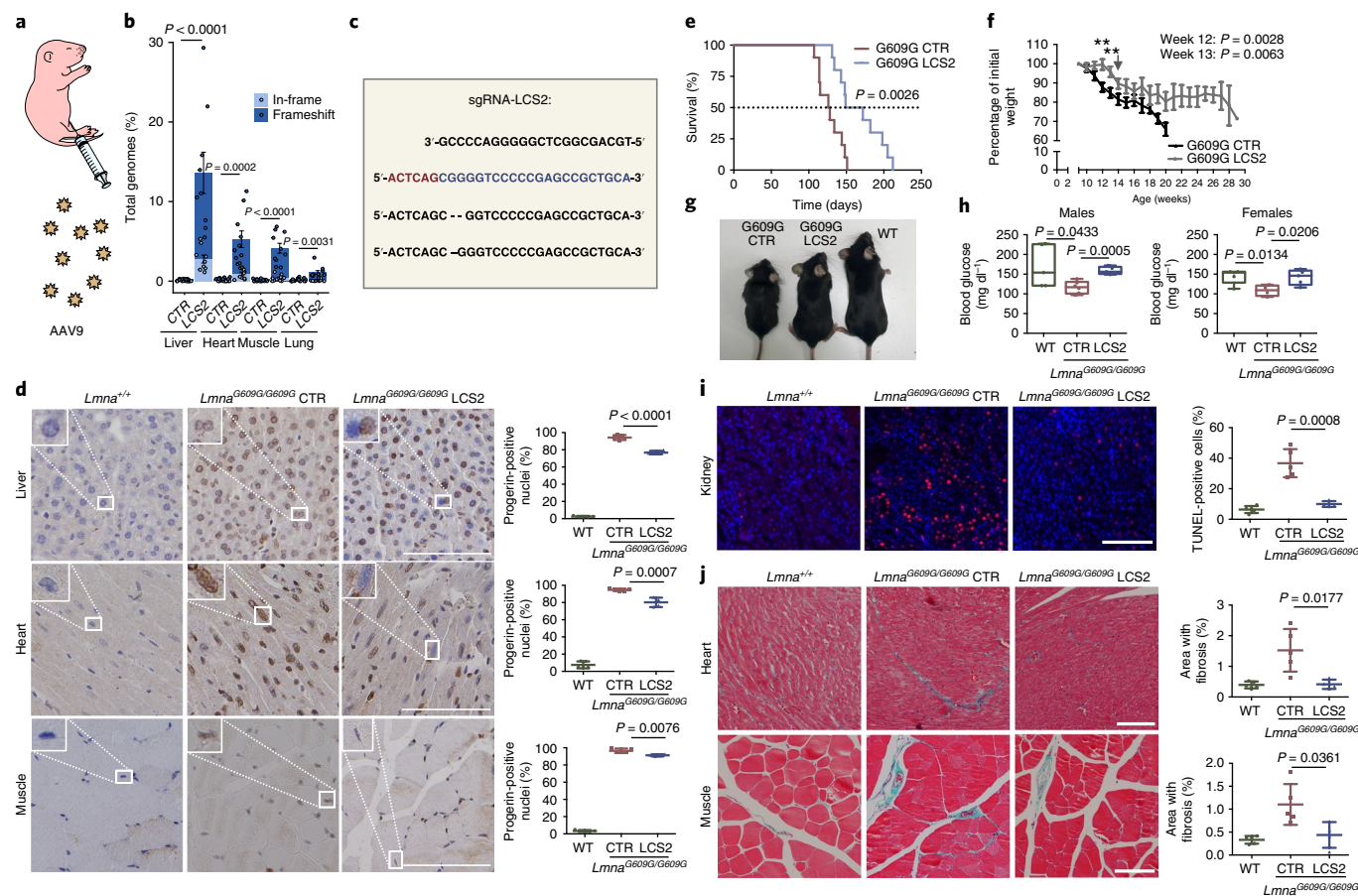


Fig. 2 | CRISPR/Cas9 delivery and phenotype amelioration in *Lmna*^{G609G/G609G} mice. **a, Intrapерitoneal injection of AAV9 in P3 mice. **b**, Percentage of in-frame and frameshift mutations at the *Lmna* target region in liver, heart, muscle and lung. Data are mean \pm s.e.m. ($n = 10$ tissues per group, except $n = 9$ sgRNA-LCS2-transduced liver; two-tailed Student's *t*-test for total indels). **c**, Alignment of the most common indels in sgRNA-LCS2-transduced mice. Blue, target sequence; red, PAM sequence. **d**, Progerin immunohistochemistry of liver, heart and muscle from WT and *Lmna*^{G609G/G609G} sgRNA-control-transduced or sgRNA-LCS2-transduced mice. Data are mean \pm s.d. ($n = 5$ WT and sgRNA-control-transduced mice; $n = 4$ sgRNA-LCS2-transduced mice; two-tailed Student's *t*-test). Insets, digital magnification of a selected area. **e**, Kaplan-Meier survival plot of sgRNA-control- versus sgRNA-LCS2-transduced *Lmna*^{G609G/G609G} mice ($n = 10$ mice per group; two-sided log-rank test). **f**, Progression of body weight of mice transduced with sgRNA-control or sgRNA-LCS2, expressed as percentage of weight at 9 weeks. Vertical arrow, time point (3.5 months) at which the cohort destined for histological studies (4–5 mice per group) was sacrificed. Mean values \pm s.e.m. are represented (initial $n = 15$ sgRNA-control-transduced mice; $n = 14$ sgRNA-LCS2-transduced mice; two-tailed Student's *t*-test). **g**, Representative image of *Lmna*^{G609G/G609G} sgRNA-control-transduced, sgRNA-LCS2-transduced and WT female mice at 3.5 months of age. **h**, Glycemia in WT (males $n = 5$; females $n = 5$), sgRNA-control-transduced (males $n = 6$; females $n = 4$) and sgRNA-LCS2-transduced *Lmna*^{G609G/G609G} mice (males, $n = 5$; females, $n = 5$). Data are represented by box plots, and whiskers are minimum to maximum values (two-tailed Student's *t*-test). **i**, TUNEL assay in kidney of 3.5-month-old mice. Data are mean \pm s.d. ($n = 5$ WT and sgRNA-control-transduced mice; $n = 4$ sgRNA-LCS2-transduced mice; two-tailed Student's *t*-test). **j**, Gomori staining in 3.5-month-old *Lmna*^{G609G/G609G} mouse tissues showing moderate perivascular and interstitial fibrosis in heart and quadriceps muscle (blue areas). Data are mean \pm s.d. ($n = 5$ WT and sgRNA-control-transduced mice; $n = 4$ sgRNA-LCS2-transduced mice; two-tailed Student's *t*-test). Scale bars, 100 μ m (**d**, **i**, **j**).**

compared to sgRNA-control-transduced animals (Fig. 2d), which concurred with the DNA sequencing results. In lung, kidney and aorta, no reduction in the number of progerin-positive nuclei was observed, possibly due to the lower tropism of AAV9 in these organs (Extended Data Fig. 5). Given the importance of vascular alterations in HGPS, the lack of noticeable direct effects on the aorta is a setback of the approach tested. Nevertheless, vascular pathologies characteristic of HGPS such as atherosclerosis are strongly influenced by systemic factors. Therefore, a reliable assessment of potential vascular benefits will require the use of susceptible mouse models carrying additional genetic alterations, such as *Apoe* or *Ldlr* inactivation.

Importantly, progerin reduction in AAV9-sgRNA-LCS2-transduced mice was translated into an increase in their median survival of 33.5 days, from 127 to 160.5 days, compared to the

sgRNA-control-transduced cohort, which represents a 26.4% lifespan increase (Fig. 2e; Extended Data Fig. 6). Mean survival was extended from 128.1 days (s.d. 15.73; 95% confidence interval 116.8–139.4) to 167.4 days (s.d. 30.41; 95% confidence interval 145.6–189.2). Likewise, maximum survival was extended from 151 to 212 days ($P = 0.0163$; one-tailed Fisher exact test) (Fig. 2e). Phenotypically, sgRNA-LCS2-transduced *Lmna*^{G609G/G609G} mice presented a healthier appearance, with retarded loss of grooming, slightly improved body weight and increased blood glucose levels, partially rescuing the hypoglycemia characteristic of these mice (Fig. 2f–h; Extended Data Figs. 7 and 8). Likewise, terminal deoxynucleotidyl transferase dUTP nick end labeling (TUNEL) analysis revealed that this group presented significantly fewer apoptotic cells in the kidney (Fig. 2i). Since progerin reduction was not detected in this organ, this suggests an effect dependent on systemic factors.

We also observed a slight decrease in gastric mucosa atrophy (Extended Data Fig. 9) and reduced focal and perivascular fibrosis in heart and quadriceps muscle in sgRNA-LCS2-transduced compared to sgRNA-control-transduced mice, in accordance with the higher mobility of the former group (Fig. 2j; Supplementary Video 1).

Antisense oligonucleotides blocking the aberrant splicing of *LMNA* transcripts have been proposed for the treatment of progeria^{5,16}. However, a longer-term therapy would be desirable. Here, we present a CRISPR/Cas9-based permanent genome-editing approach that targets *LMNA* exon 11, specifically interfering with lamin A/progerin expression. Because the Cas9 endonuclease is not directed specifically against the p.Gly608Gly point mutation, this strategy could also be applicable to laminopathies caused by other *LMNA* mutations¹⁷. However, although lamin A is dispensable in cells and mice^{5,6}, the consequences of abrogating its expression in humans remain unexplored. Therefore, alternative CRISPR/Cas9-based systems, such as base editors¹⁸, also need to be tested. The coexistence of progeroid and normal cells at a ratio of approximately 50/50 in mosaic mice resulted in a completely normal phenotype and lifespan¹⁴. In the current work, although the editing efficiency is lower, extensive phenotype amelioration and lifespan extension were obtained. The extent to which the modest editing efficiency attained is due to low delivery efficacy could not be determined reliably, as the packaging limit of the vector precluded the inclusion of a suitable reporter. Interestingly, the concurrent study by Beyret and colleagues¹⁹ describes another successful CRISPR/Cas9-based treatment of the *Lmna*^{G609G/G609G} mouse model of HGPS. Nevertheless, further research on putative off-target events and adverse effects of the Cas9 nuclease will be needed to ensure the safety of this intervention. Regardless of these limitations, these two studies show the preclinical efficacy of genome editing in a mouse model of progeria and pave the way for using CRISPR/Cas9 in HGPS and other currently incurable systemic diseases.

Online content

Any methods, additional references, Nature Research reporting summaries, source data, statements of data availability and associated accession codes are available at <https://doi.org/10.1038/s41591-018-0338-6>.

Received: 22 January 2018; Accepted: 18 December 2018;
Published online: 18 February 2019

References

1. Hennekam, R. C. *Am. J. Med. Genet. A.* **140**, 2603–2624 (2006).
2. De Sandre-Giovannoli, A. et al. *Science* **300**, 2055 (2003).
3. Eriksson, M. et al. *Nature* **423**, 293–298 (2003).

4. Goldman, R.D. et al. *Proc. Natl. Acad. Sci. USA* **101**, 8963–8968 (2004).
5. Osorio, F. G. et al. *Sci. Transl. Med.* **3**, 106ra107 (2011).
6. Fong, L. G. et al. *J. Clin. Invest.* **116**, 743–752 (2006).
7. Gordon, L. B., Rothman, F. G., Lopez-Otin, C. & Misteli, T. *Cell* **156**, 400–407 (2014).
8. Gordon, L. B. et al. *Circulation* **130**, 27–34 (2014).
9. Gordon, L. B. et al. *JAMA* **319**, 1687–1695 (2018).
10. Amoasii, L. et al. *Sci. Transl. Med.* **9**, eaan8081 (2017).
11. Yang, Y. et al. *Nat. Biotechnol.* **34**, 334–338 (2016).
12. Gao, X. et al. *Nature* **553**, 217–221 (2018).
13. Doudna, J. A. & Charpentier, E. *Science* **346**, 1258096 (2014).
14. de la Rosa, J. et al. *Nat. Commun.* **4**, 2268 (2013).
15. Ran, F. A. et al. *Nature* **520**, 186–191 (2015).
16. Scaffidi, P. & Misteli, T. *Nat. Med.* **11**, 440–445 (2005).
17. Bar, D. Z. et al. *J. Med. Genet.* **54**, 212–216 (2017).
18. Gaudelli, N. M. et al. *Nature* **551**, 464–471 (2017).
19. Beyret, E. et al. *Nat. Med.* <https://doi.org/10.1038/s41591-019-0343-4> (2019).

Acknowledgements

We thank G. Velasco, R. Villa-Belosta, C. Bárcena, A.P. Ugalde and X.M. Caravia for helpful comments and advice, and R. Feijoo, A. Moyano, D.A. Puente and S.A. Miranda for excellent technical assistance. We also acknowledge the generous support by J.I. Cabrera and Associazione Italiana Progeria Sammy Basso and the contribution of Dr. Matthew Golding to the generation of the anti-murine progerin antibody. The Instituto Universitario de Oncología del Principado de Asturias is supported by Fundación Bancaria Caja de Ahorros de Asturias. J.M.P.F. is supported by Ministerio de Economía y Competitividad (MINECO/FEDER: No. SAF2015-64157-R) and Gobierno del Principado de Asturias. C.L.-O. is supported by grants from the European Research Council (ERC-2016-ADG, DeAge), Ministerio de Economía y Competitividad (MINECO/FEDER: Nos. SAF2014-52413-R and SAF2017-87655-R), Instituto de Salud Carlos III (RTICC) and Progeria Research Foundation (No. PRF2016-66). O.S.-F. is recipient of an FPU fellowship. A.R.F. is recipient of a Ramón y Cajal fellowship. The generation of progerin antibody was funded by the Wellcome Trust (No. 098291/Z/12/Z to S.N.).

Author contributions

F.G.O., J.M.P.F. and C.L.-O. conceived and designed experiments. O.S.-F., F.G.O., V.Q., F.R., S.B., D.M. and A.R.F. performed experiments and analyzed data. L.R., A.B. and S.N. provided reagents. O.S.-F., F.G.O., A.R.F., J.M.P.F. and C.L.-O. wrote the manuscript. All authors revised the manuscript.

Competing interests

The authors declare no competing interests.

Additional information

Extended data is available for this paper at <https://doi.org/10.1038/s41591-018-0338-6>.

Supplementary information is available for this paper at <https://doi.org/10.1038/s41591-018-0338-6>.

Reprints and permissions information is available at www.nature.com/reprints.

Correspondence and requests for materials should be addressed to J.M.P.F. or C.L.

Publisher's note: Springer Nature remains neutral with regard to jurisdictional claims in published maps and institutional affiliations.

© The Author(s), under exclusive licence to Springer Nature America, Inc. 2019

Methods

Plasmids and sgRNA cloning. All sgRNA-LCS were designed to target exon 11 of the *LMNA* gene using the Benchling CRISPR Design tool. For infections involving human and mouse fibroblasts, we used the lentiviral vector lentiCRISPRv2 (Addgene) in which we cloned the sgRNA-control (5'-GGAGACGGGATACCGTCTCT-3') or the sgRNA-LCS1 (5'-AGCGCAGGTTGACTCAGCG-3'). For AAV injection, we cloned the sgRNA-control or sgRNA-LCS2 (5'-GTGCAGCGGCTCGGGGACCCCG-3') in the pX601-AAV vector from Addgene, containing the Cas9 nuclease from *S. aureus*.

Virus production. pX601-sgRNA-control or pX601-sgRNA-LCS2 plasmids were packaged as AAV serotype 9 by The Viral Vector Production Unit of the Universitat Autònoma de Barcelona (Barcelona, Spain), followed by polyethylene glycol precipitation and iodixanol gradient purification. Aliquots of 2×10^{11} genome copies in 60 μ l of phosphate buffered saline (PBS)-MK were prepared for the injections.

Animal experiments. All animal experiments were performed in accordance with institutional guidelines and were approved by the Committee of Animal Experimentation of University of Oviedo (Oviedo, Spain). For AAV injection, P3 *Lmna*^{G609G/G609G} mice were injected intraperitoneally with either sgRNA-control- or sgRNA-LCS2-containing vectors. All gene-editing and phenotypic analyses were performed at 3.5 months of age. To analyze blood glucose, animals were starved overnight and glucose levels were measured with an Accu-Check glucometer (Roche Diagnostics) using blood from the tail vein.

Histological analysis and TUNEL staining. Tissues were collected in 4% paraformaldehyde in PBS and embedded in paraffin. Hematoxylin and eosin (H&E) staining was performed on stomach tissue, and atrophy of the gastric mucosa was blindly evaluated by a pathologist on three different sections per mouse, establishing a pathological score (0, normal; 1, mild; 2, moderate; 3, severe atrophy). TUNEL staining in mouse kidneys was done according to the manufacturer's instructions (In-Situ Cell Death Detection Kit, TMR red, Roche). To determine the number of TUNEL-positive nuclei, ten random fields per mouse were blindly analyzed using ImageJ. H&E with Gomori's trichrome staining was performed in heart and quadriceps muscle, and five random fields per tissue were quantified with a FIJI plugin provided by A. M. Nistal (Servicios Científico-Técnicos, Universidad de Oviedo).

Illumina sequencing and bioinformatic analysis. MiSeq DNA sequencing was performed by Macrogen, using the Illumina 300bpPE. To prepare the library, DNA was isolated from liver, heart, muscle and lung from mice transduced with sgRNA-control- or sgRNA-LCS2-encoding AAVs. Next, we amplified the target region of the Cas9 nuclease with the *Pfu* DNA polymerase (Promega) adding the Illumina adapters by two PCR: NGS1_fwd: ACACCTCTTCCCCTACACGACGCTCTTC-CGATCTNNNTGTGACACTGGAGGCAAG and NGS1_rev: GTGACTG-GAGTTCAGACGTGTGCTCTCCGATCTCAAGTCCCATCACTGGTT for the first PCR, and NGS2_fwd: AATGATACGGCGACCCGAGATCTACACTTCCCCTACACGACGCTCTCCGATCT and NGS2_rev: CAAGCAGAAGACGGCATAACGAGATXXXXXXGTGACTGGAGTTC for the second PCR. The N represents random bases and the X the sequence used for the index. Genomic reads in FASTQ format were aligned to the GRCh38.p6 assembly of the mouse genome using BWA v. 0.7.5a-r405 (ref. ²⁰). Then, reads spanning the genomic region putatively affected by the CRISPR/Cas9 action (chr3: 88482555-88482615) were extracted with Samtools v. 1.3.1 (ref. ²¹) and analyzed using in-house Perl scripts. Briefly, these scripts isolate the part of each read spanning the chosen region, highlight small insertions/deletions and output a count of each regional sequence. We then analyzed the percentage of the sequences showing regional differences in sgRNA-control- and sgRNA-LCS2-transduced mouse samples.

Capillary electrophoresis-based fragment analysis. We performed PCR amplification of the target region with the forward oligonucleotide labeled with 6FAM fluorophore in the 5' position, facilitating fragment analysis of the resulting products by capillary electrophoresis. For human cells, we used the oligonucleotides HsLMNA_Fwd: [6FAM] GCACAGAACCACCTTCT and HsLMNA_Rev: TGACCAGATTGTCCTCCCAAG, while for mouse cells we used MmLmna_Fwd: [6FAM] GTCCCCATCACTGGTTGTC and MmLmna_Rev: TGACTAGGTTGTCCTCCGAAG.

Cell culture, transfection and viral transduction. We maintained HEK-293T cell cultures in Dulbecco's modified Eagle's medium supplemented with 10% fetal bovine serum, 1% penicillin-streptomycin-L-glutamine and 1% antibiotic-antimycotic (Gibco) at 37 °C in 5% CO₂. In the case of human and mouse fibroblasts, $\times 1$ non-essential amino acids, 10 mM HEPES buffer, 100 μ M 2-mercaptoethanol and $\times 1$ sodium pyruvate (Gibco) were also added to the previous medium and 15% fetal bovine serum was used. For lentiviral infection, HEK-293T cells were transfected with lentiCRISPRv2 vector together with

second-generation packaging plasmids using Lipofectamine reagent (Life Technologies). Supernatants were filtered through 0.45 μ m polyethersulfone filters to collect the viral particles, and added at 1:3 dilution to previously seeded human and mouse fibroblasts supplemented with 0.8 μ g ml⁻¹ of polybrene (Millipore). Selection with puromycin (2 μ g ml⁻¹) was performed 2 days after infection, and the editing efficiency and nuclear aberrations were quantified one week later.

RNA preparation and RT-qPCR. Collected cells or tissues were homogenized in TRIzol reagent (Life Technologies) and RNA was extracted with the RNeasy Mini kit following the manufacturer's instructions (QIAGEN). cDNA was synthesized with the QuantiTect Reverse Transcription kit (QIAGEN) using 1 μ g of total RNA, and then RT-qPCR analysis of mouse tissues was performed. For progerin analysis, TaqMan PCR Universal Mastermix (Applied Biosystems) and the following oligonucleotides and probe were used: MmProgerin_fwd (5'-TGAGTACAACCTGCGCTCAC-3'), MmProgerin_rev (5'-TGGCAGGTCCCAGATTACAT-3') and MmProgerin_probe (5'-CGGGAGCCCAGAGCTCCCAGAA-3'); using a β -actin (Applied Biosystems) as endogenous control. For lamin C analysis, we used SYBR green PCR Universal Mastermix (Applied Biosystems) and the oligonucleotides Lmnc_fwd (5'-CGACGAGGATGGAGAAGAGC-3') and Lmnc_rev (5'-AGACTTTGGCATGGAGGTGG-3') for lamin C; or Actb_Fwd (5'-CTGAGGAGCACCTGTGCT-3') and Actb_Rev (5'-GTTGAAGGTCTCAAACATGATCTG-3') for β -actin as endogenous control.

Protein isolation and immunoblot analysis. Cells were washed with $\times 1$ PBS and homogenized in RIPA lysis buffer containing 100 mM Tris pH 7.4, 150 mM NaCl, 10 mM EDTA pH 8.0, 1% sodium deoxycholate, 1% Triton X-100 and 0.1% sodium dodecyl sulfate (SDS), supplemented with protease inhibitor cocktail (Complete, EDTA-free, Roche) and phosphatase inhibitors (PhosSTOP, Roche). Protein concentration was determined with the Pierce BCA Protein Assay Kit, and 30 μ g per lane were loaded onto 8% SDS-polyacrylamide gels. Gels were then transferred to nitrocellulose membranes, blocked with 5% nonfat dry milk in TBS-T buffer (20 mM Tris pH 7.4, 150 mM NaCl and 0.05% Tween 20) and incubated overnight at 4 °C with primary antibodies: 1:500 mouse monoclonal anti-lamin A/C (MANLAC1, provided by G. Morris) for experiments involving mouse cells, 1:1,000 rabbit polyclonal anti-lamin A/C (sc-20681, Santa Cruz Biotechnology) for experiments involving human cells or 1:10,000 anti- β -actin (AC-15, Sigma) as an endogenous control. Finally, blots were incubated with 1:10,000 goat anti-mouse (Jackson ImmunoResearch) or 1:3,000 goat anti-rabbit horseradish peroxidase (HRP) (Cell Signaling) in 1.5% nonfat dry milk in TBS-T and washed with TBS-T. Immunoreactive bands were developed with Immobilon Western chemiluminescent HRP substrate (Millipore) in a LAS-3000 Imaging System (Fujifilm). Bands were quantified using ImageJ.

Immunofluorescence, immunohistochemistry and nuclear morphology analysis. For immunofluorescence assays, cells were fixed in 4% paraformaldehyde solution, rinsed in PBS and permeabilized with 0.5% Triton X-100. Afterwards, they were blocked with 15% goat serum solution and incubated overnight at 4 °C with a rabbit polyclonal anti-progerin antibody in PBS (1:200). Next, slides were washed with TBS-T and incubated with 1:500 anti-rabbit secondary antibody Alexa Fluor 488 (Life Technologies). Nuclei were stained with 4',6-diamidino-2-phenylindole (DAPI, Invitrogen). In the case of immunohistochemical analysis, tissues were fixed in 4% paraformaldehyde solution and incubated with Target Retrieval Solution at 95 °C for 20 min, Peroxidase Blocking Solution for 5 min and Protein Block Serum Free (all from Dako) for 20 min before incubation with the anti-progerin primary antibody (1:300 dilution) for 1 h. An HRP-conjugated polyclonal anti-rabbit was applied for 30 min and then 3,3'-diaminobenzidine for 10 min. Tissues were counterstained with hematoxylin (Dako) and visualized by light microscopy. Rabbit anti-progerin polyclonal antibody was generated using peptide immunogens and standard immunization procedures (S. Nourshargh et al., manuscript in preparation). The specificity of the antibody was confirmed by nuclear staining of *Lmna*^{G609G/G609G} mouse-derived fibroblasts, which was negative in the case of WT cells. To determine the percentage of progerin-positive cells and nuclei with aberrations, five random fields per culture or tissue sample were blindly analyzed. For tissue samples, in each field a pre-established grid was used and five random areas were quantified.

Statistical analysis. Animals of the same age were used for comparisons between mice groups, and no statistical method was used to predict sample size. For statistical analysis of differences between mouse cohorts, normality was assessed using the Shapiro-Wilk test in those cases where $n > 10$. In the remaining cases, normality was assumed based on previous data and we performed two-tailed Student's *t*-test to study the statistical significance. For survival comparisons we used the log-rank test, and differences in maximum lifespan were calculated using the one-tailed Fisher exact test comparing the number of live sgRNA-control- and sgRNA-LCS2-transduced mice at the age corresponding to the 80th percentile of lifespan in the joint survival distribution. We used Microsoft Excel or GraphPad

Prism software for the analysis, and significant differences were considered when $*P < 0.05$, $**P < 0.01$, $***P < 0.001$.

Reporting Summary. Further information on research design is available in the Life Sciences Reporting Summary attached to this paper.

Code availability

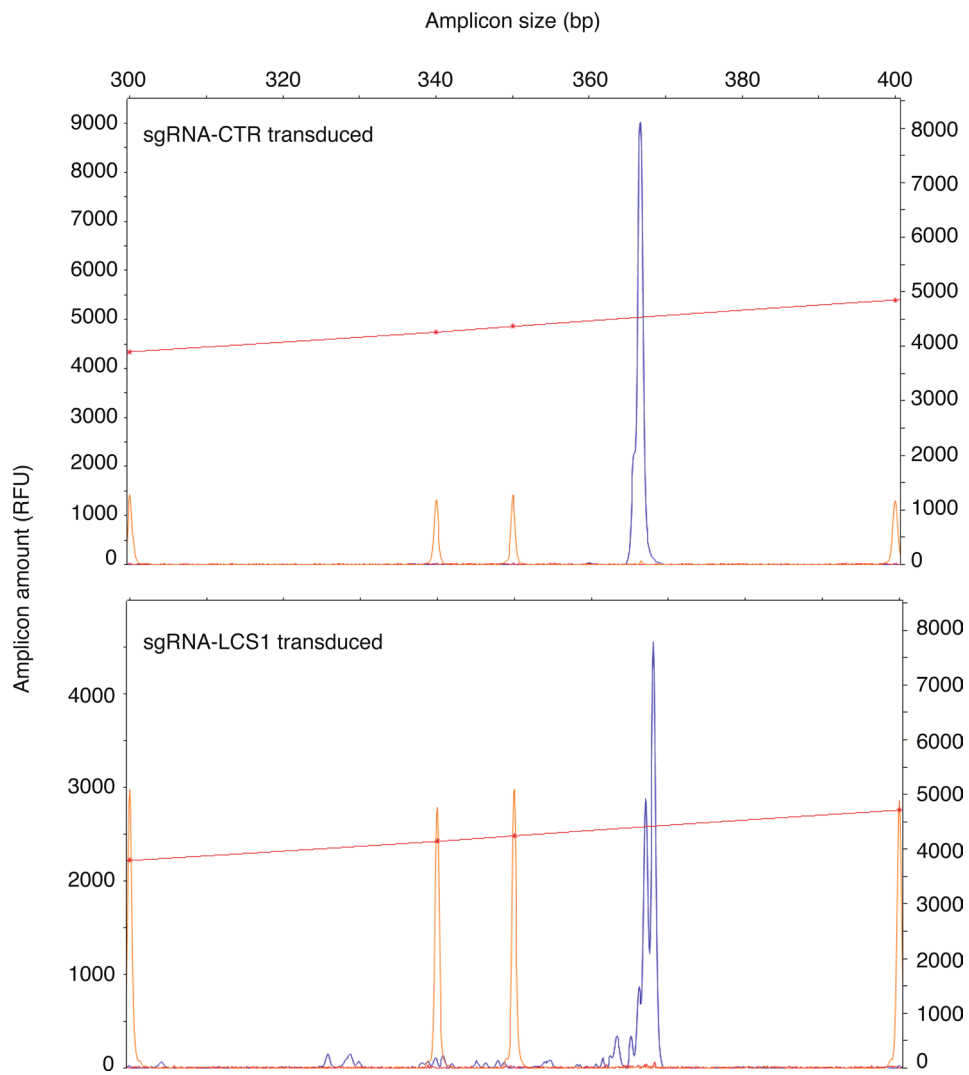
The in-house Perl scripts used for gene edition analysis can be freely downloaded at <https://github.com/vqf/genotypes>.

Data availability

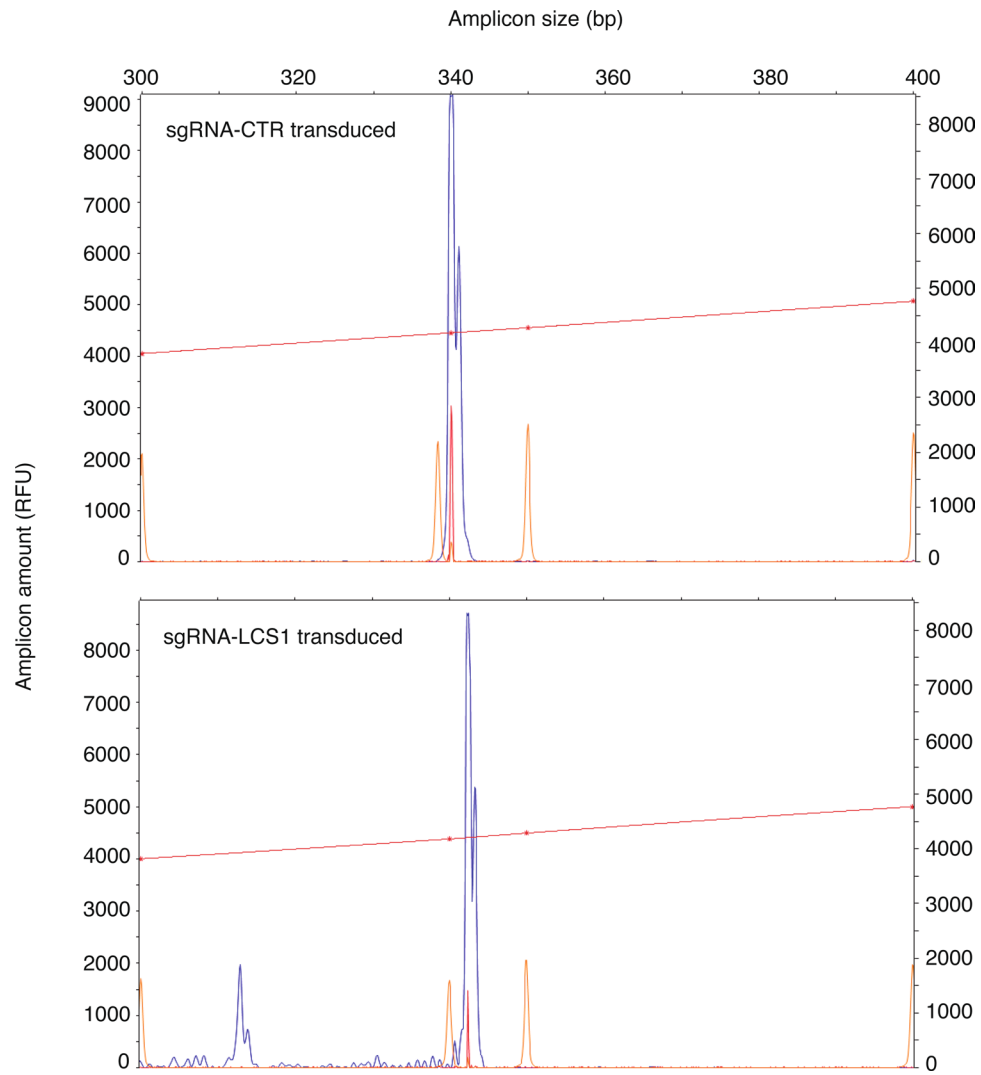
The MiSeq data were deposited in the NCBI SRA (no. [PRJNA505974](https://www.ncbi.nlm.nih.gov/sra/PRJNA505974)). Other data from this study are available from the corresponding authors. Any materials that can be shared will be released via a Material Transfer Agreement.

References

- Li, H. & Durbin, R. *Bioinformatics* **26**, 589–595 (2010).
- Li, H. et al. *Bioinformatics* **25**, 2078–2079 (2009).

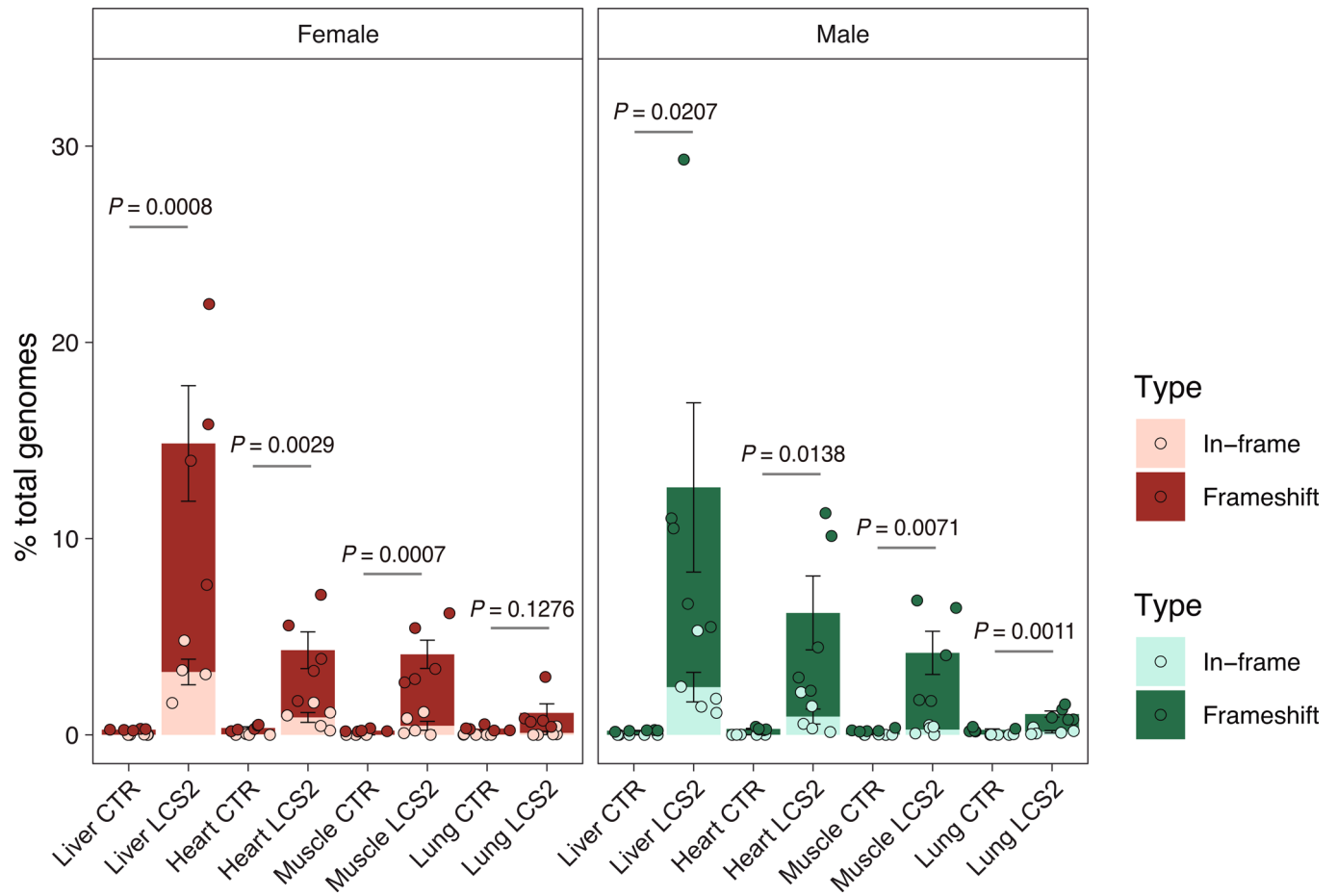


Extended Data Fig. 1 | Representative capillary electrophoresis-based fragment analysis of sgRNA-control- and sgRNA-LCS1-transduced *Lmna*^{G609G/G609G} mouse embryonic fibroblasts ($n = 3$ independent infections and MEF lines). Red line and orange peaks correspond to size standards.

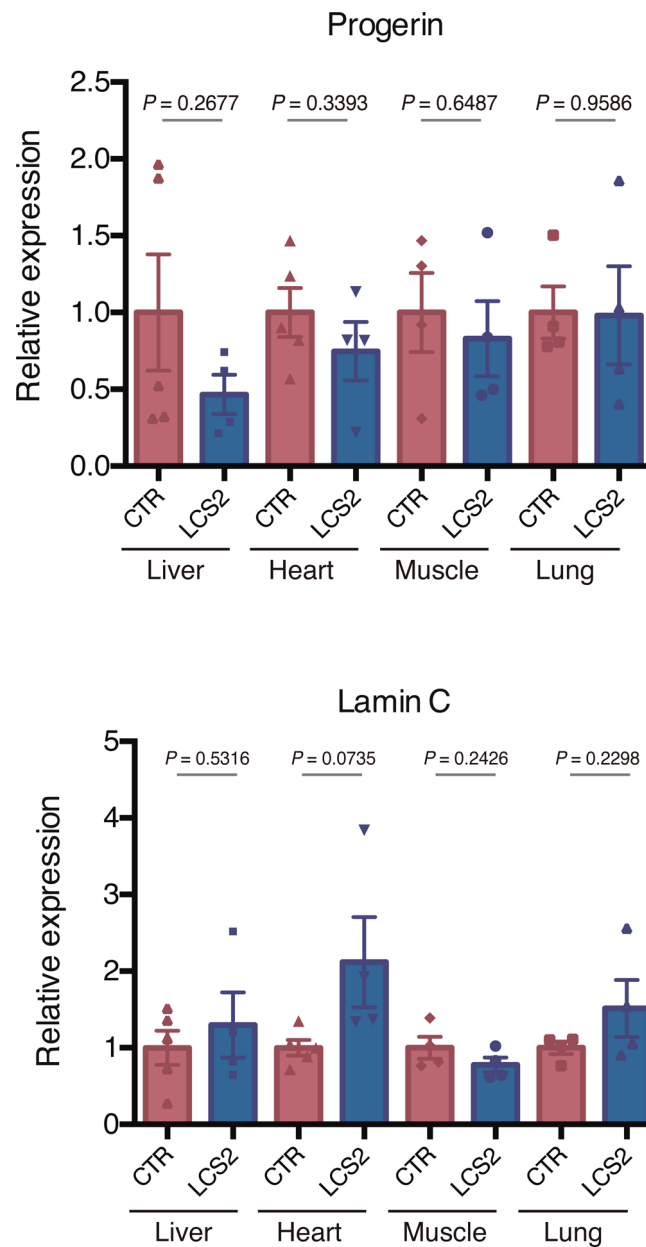


Extended Data Fig. 2 | Representative capillary electrophoresis-based fragment analysis of sgRNA-control- and sgRNA-LCS1-transduced *LMNA*^{G608G/+} human fibroblasts ($n = 3$ independent infections). Red line and orange peaks correspond to size standards.

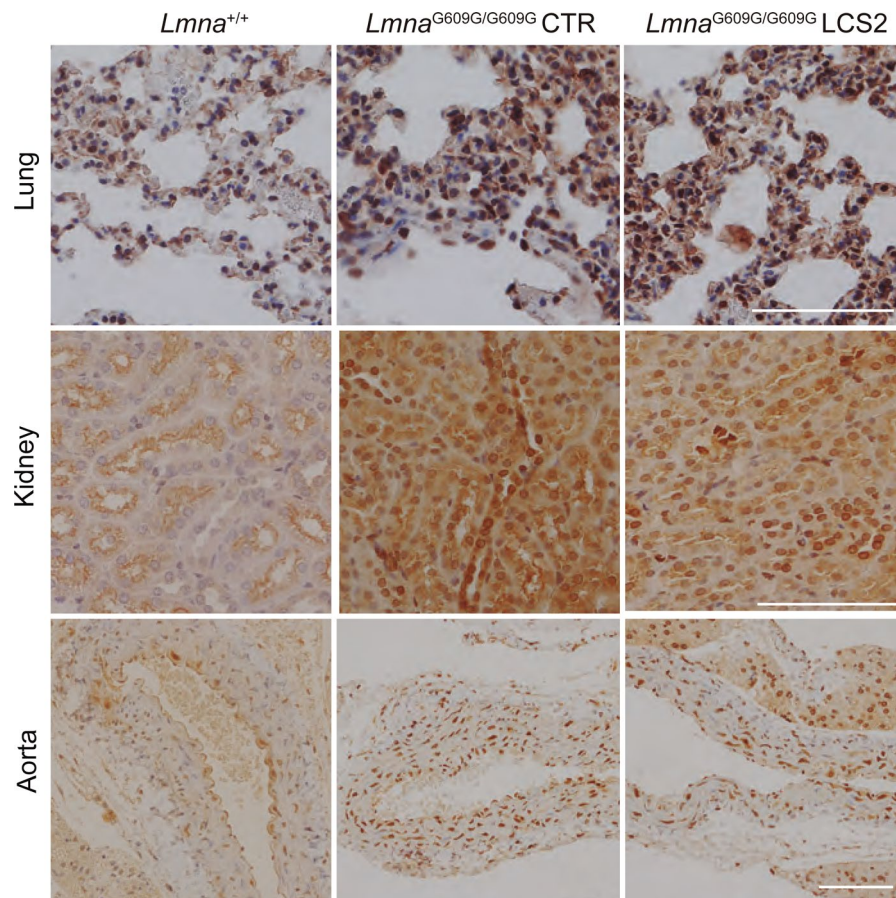
Editing efficiency



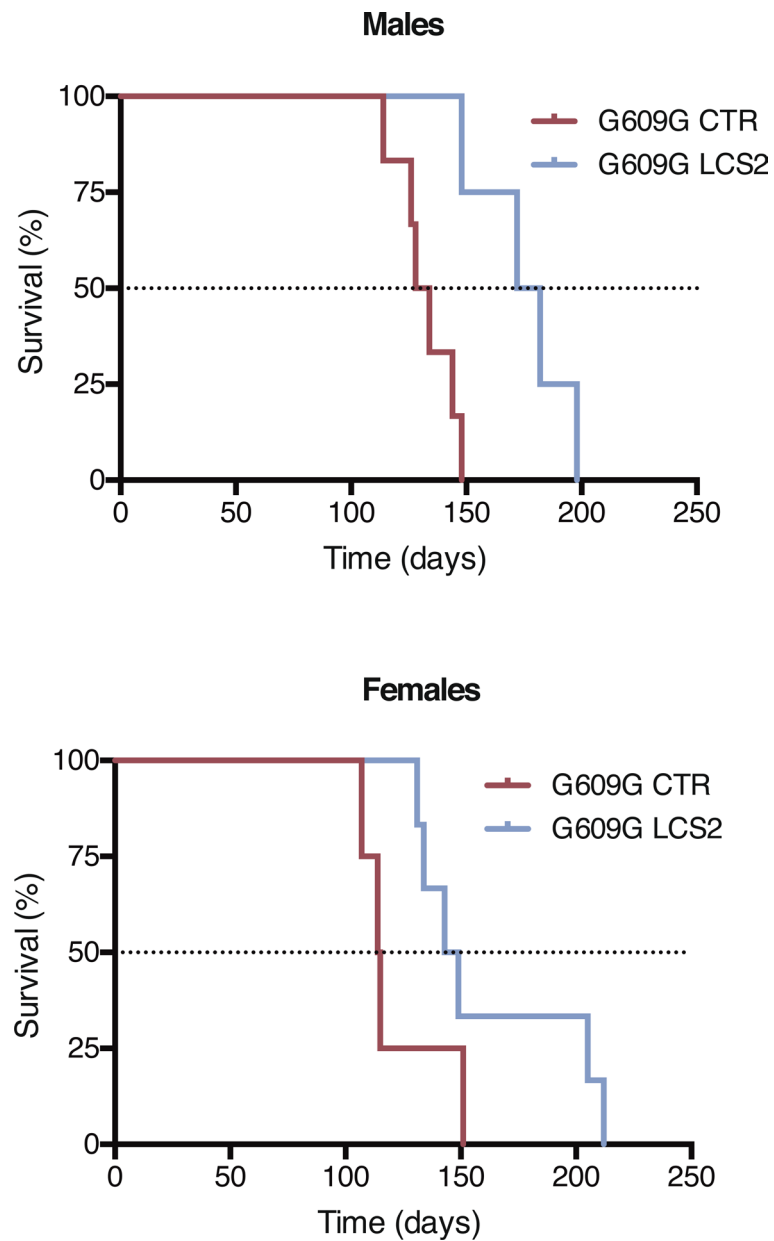
Extended Data Fig. 3 | Percentage of indels in *Lmna*^{G609G/G609G} sgRNA-LC2-transduced male and female mouse tissues. Data are mean ± s.e.m. (n=5 tissues per group, except in sgRNA-LCS2-transduced female liver where n=4; two-tailed Student's t-test).



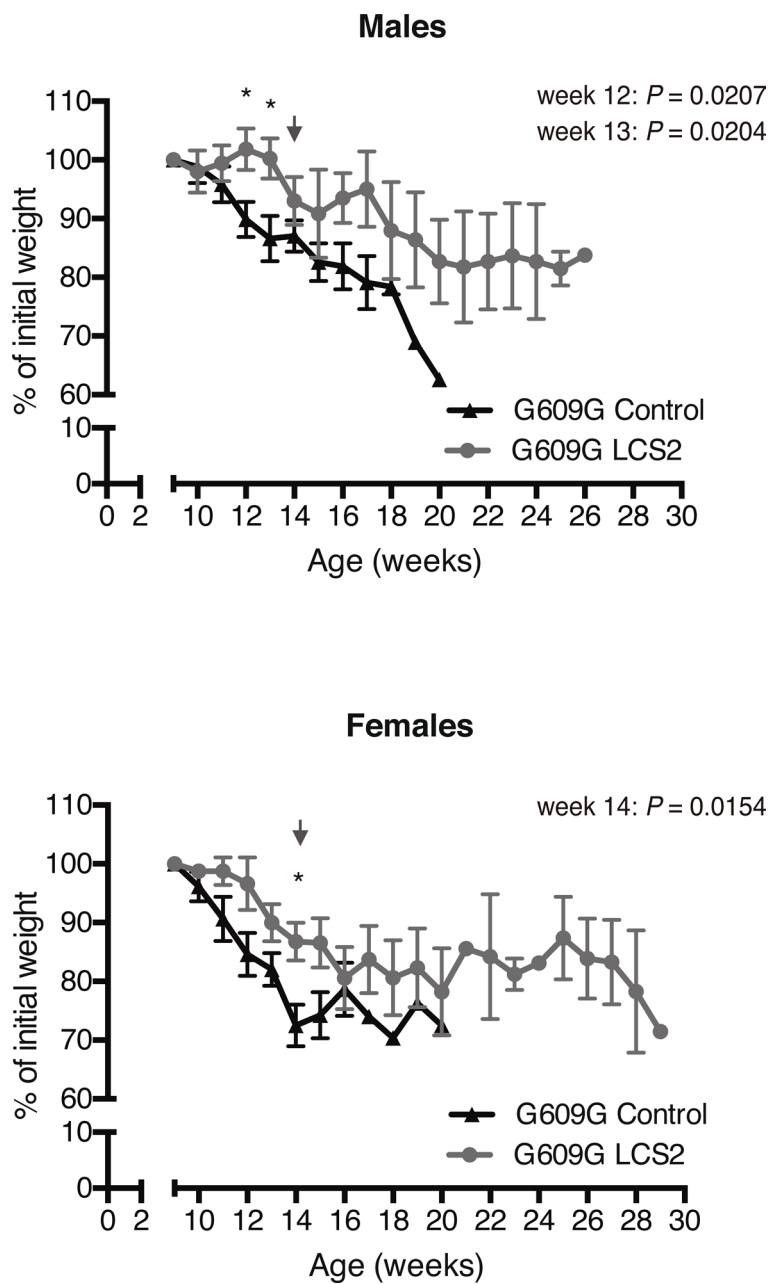
Extended Data Fig. 4 | RT-qPCR analysis of progerin and lamin C in tissues from *Lmna*^{G609G/G609G} sgRNA-control-transduced and *Lmna*^{G609G/G609G} sgRNA-LCS2-transduced mice. Data are mean \pm s.e.m. ($n=4$ tissues per group, except sgRNA-control-transduced liver and heart where $n=5$; two-tailed Student's t -test).



Extended Data Fig. 5 | Progerin immunohistochemistry in lung, kidney and aorta from WT, *Lmna*^{G609G/G609G} sgRNA-control-transduced and *Lmna*^{G609G/G609G} sgRNA-LCS2-transduced mice (lung and kidney, $n = 5$ for WT and sgRNA-control-transduced mice and $n = 4$ for sgRNA-LCS2-transduced mice; aorta, $n = 2$ for WT and $n = 3$ for sgRNA-control- and sgRNA-LCS2-transduced *Lmna*^{G609G/G609G} mice). Scale bar, 100 μm .



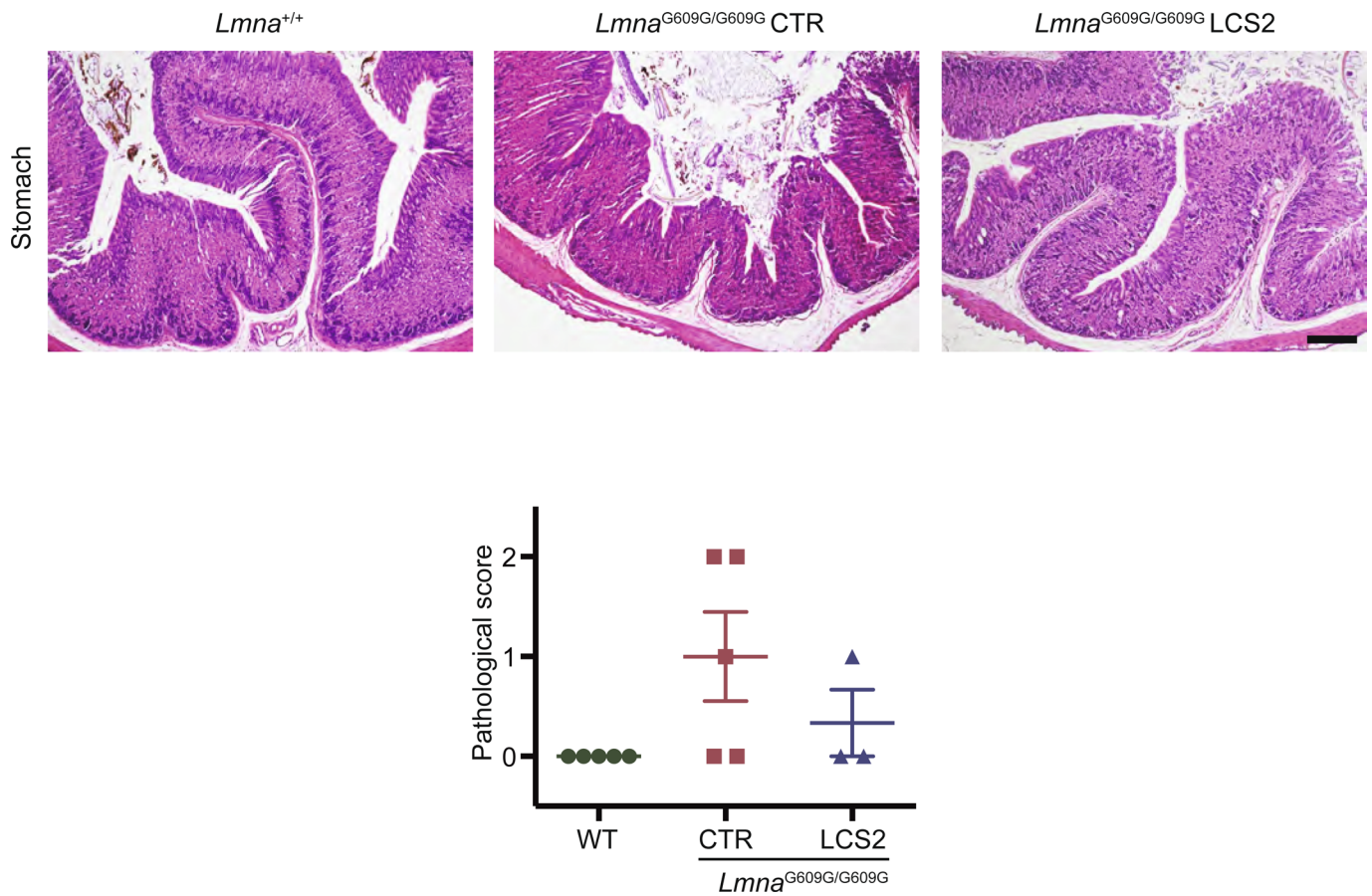
Extended Data Fig. 6 | Kaplan-Meier survival plot of *Lmna*^{G609G/G609G} male and female mice transduced with sgRNA-control ($n=6$ males; $n=4$ females) or sgRNA-LCS2 ($n=4$ males; $n=6$ females).



Extended Data Fig. 7 | Progression of body weight of male and female mice transduced with sgRNA-control or sgRNA-LCS2, expressed as percentage of weight at 9 weeks. Mean values \pm s.e.m. are shown (for males, initial $n = 9$ sgRNA-control-transduced mice and $n = 8$ sgRNA-LCS2-transduced mice; for females, initial $n = 6$ mice per group; two-tailed Student's t -test). Vertical arrow indicates the time point (3.5 months) at which the cohort destined for histological studies was sacrificed.



Extended Data Fig. 8 | Images of three sex- and age-matched mice transduced with the sgRNA-LCS2 compared to sgRNA-control-transduced animals.



Extended Data Fig. 9 | H&E staining of gastric mucosa from WT, *Lmna*^{G609G/G609G} sgRNA-control-transduced and *Lmna*^{G609G/G609G} sgRNA-LCS2-transduced mice. The graph shows atrophy quantification according to a pathological score as described in Methods. Data are mean ± s.e.m. ($n = 5$ for WT and sgRNA-control-transduced mice; $n = 3$ for sgRNA-LCS2-transduced mice).

Life Sciences Reporting Summary

Nature Research wishes to improve the reproducibility of the work that we publish. This form is intended for publication with all accepted life science papers and provides structure for consistency and transparency in reporting. Every life science submission will use this form; some list items might not apply to an individual manuscript, but all fields must be completed for clarity.

For further information on the points included in this form, see [Reporting Life Sciences Research](#). For further information on Nature Research policies, including our [data availability policy](#), see [Authors & Referees](#) and the [Editorial Policy Checklist](#).

Please do not complete any field with "not applicable" or n/a. Refer to the help text for what text to use if an item is not relevant to your study. For final submission: please carefully check your responses for accuracy; you will not be able to make changes later.

▶ Experimental design

1. Sample size

Describe how sample size was determined.

Sample size was determined based on previous experiments of our laboratory, carried out with the same animal model under identical environmental conditions.

2. Data exclusions

Describe any data exclusions.

Two AAV9-treated mice (one from the control cohort and another one from the sgRNA-LCS2 group) were excluded from the survival plot due to perinatal death. This event could be explained by an early manipulation and a higher frailty of progeroid mice. The analysis of indel mutations in the liver of a LCS2-transduced mouse was also excluded due to a low number of reads in NGS (only 24 reads compared to more than 100,000 in the rest of analyzed samples). These exclusion criteria had not been pre-established.

3. Replication

Describe the measures taken to verify the reproducibility of the experimental findings.

Three independent infections were done for in vitro experiments. All attempts at replication were successful.

4. Randomization

Describe how samples/organisms/participants were allocated into experimental groups.

Allocation of both mice and cell cultures to each group was random.

5. Blinding

Describe whether the investigators were blinded to group allocation during data collection and/or analysis.

Nuclear abnormalities and progerin analysis in cultures were quantified by investigators who were blinded to the identity of the analyzed cells. In the same way, histological analysis (Gomori staining, TUNEL assay and progerin immunohistochemistry) were also performed by investigators blinded to group identity.

Note: all in vivo studies must report how sample size was determined and whether blinding and randomization were used.

6. Statistical parameters

For all figures and tables that use statistical methods, confirm that the following items are present in relevant figure legends (or in the Methods section if additional space is needed).

n/a Confirmed

- The exact sample size (n) for each experimental group/condition, given as a discrete number and unit of measurement (animals, litters, cultures, etc.)
- A description of how samples were collected, noting whether measurements were taken from distinct samples or whether the same sample was measured repeatedly
- A statement indicating how many times each experiment was replicated
- The statistical test(s) used and whether they are one- or two-sided
Only common tests should be described solely by name; describe more complex techniques in the Methods section.
- A description of any assumptions or corrections, such as an adjustment for multiple comparisons
- Test values indicating whether an effect is present
Provide confidence intervals or give results of significance tests (e.g. P values) as exact values whenever appropriate and with effect sizes noted.
- A clear description of statistics including central tendency (e.g. median, mean) and variation (e.g. standard deviation, interquartile range)
- Clearly defined error bars in all relevant figure captions (with explicit mention of central tendency and variation)

See the web collection on [statistics for biologists](#) for further resources and guidance.

► Software

Policy information about [availability of computer code](#)

7. Software

Describe the software used to analyze the data in this study.

-Microsoft Excel v. 15.21.1 and GraphPad Prism v. 6.0.2 were used for the statistical analysis.
-BWA v. 0.7.5a-r405 and Samtools v. 1.3.1 were used for MiSeq analysis.
-ImageJ v. 1.48v was used for Western blot and TUNEL analysis.
-FIJI v. 1.52i was used for Gomori quantification.

For manuscripts utilizing custom algorithms or software that are central to the paper but not yet described in the published literature, software must be made available to editors and reviewers upon request. We strongly encourage code deposition in a community repository (e.g. GitHub). [Nature Methods guidance for providing algorithms and software for publication](#) provides further information on this topic.

► Materials and reagents

Policy information about [availability of materials](#)

8. Materials availability

Indicate whether there are restrictions on availability of unique materials or if these materials are only available for distribution by a third party.

Unique materials used are available from the authors upon Material Transfer Agreement signature. AAVs were obtained from The Viral Vector Production Unit (UPV) of the Universitat Autònoma de Barcelona (Barcelona, Spain).

9. Antibodies

Describe the antibodies used and how they were validated for use in the system under study (i.e. assay and species).

The primary antibodies used were:
-Mouse monoclonal anti-lamin A/C (MANLAC1) was provided by Prof. Glenn Morris (Wolfson Centre for Inherited Neuromuscular Disease, UK) and used at a dilution 1:500. For validation, cultured mouse fibroblast cell extracts were used.
-Rabbit polyclonal anti-lamin A/C (H-110; cat: sc-20681) from Santa Cruz Biotechnology was used at a dilution 1:1,000. According to the websites of the manufacturer, this antibody reacts against Lamin A/C from mouse, rat and human origin.
-Mouse monoclonal anti-beta-actin (AC-15; cat: A5441; lot: 014M4759) was purchased from Sigma and used at a dilution 1:10,000. According to the websites of the manufacturer, reacts against guinea pig, canine, *Hirudo medicinalis*, feline, pig, carp, mouse, chicken, rabbit, sheep, rat, human and bovine orthologs.
-The anti-progerin polyclonal antibody was generated using peptide immunogens and standard immunization procedures (S. Nourshargh et al., manuscript in preparation). 1:200-1:300 dilutions were used and its specificity was confirmed by nuclear staining of LmnaG609G/G609G mice-derived fibroblasts, which was negative in the case of wild-type cells.

The secondary antibodies used were:
-Goat anti-mouse IgG HRP-linked antibody from Jackson ImmunoResearch (cat: 115-035-062; lot:121006) diluted 1:10,000.
-Goat anti-rabbit IgG HRP-linked antibody from Cell Signaling (cat: 7074S; lot: 27) diluted 1:3,000.
-Goat anti-rabbit IgG - H&L 488 from Alexa Fluor (cat: A11034; lot: 1670152) diluted 1:500.

10. Eukaryotic cell lines

a. State the source of each eukaryotic cell line used.

HEK-293T cells are from ATCC. Controls and progeroid mouse fibroblasts cultures were established in our laboratory from control and mutant mice. Human control and HGPS fibroblasts are from Coriell.

b. Describe the method of cell line authentication used.

The identity of control and progeroid fibroblasts was confirmed by Western blot of lamin A/C. PCR-based microsatellite characterization of HEK-293T cells was performed at the University of Oviedo.

c. Report whether the cell lines were tested for mycoplasma contamination.

The cell lines were not tested for mycoplasma contamination.

d. If any of the cell lines used are listed in the database of commonly misidentified cell lines maintained by ICLAC, provide a scientific rationale for their use.

HEK-293T cells are widely used for infection experiments. The identity of HEK-293T was assessed by PCR-based microsatellite characterization.

► Animals and human research participants

Policy information about [studies involving animals](#); when reporting animal research, follow the [ARRIVE guidelines](#)

11. Description of research animals

Provide all relevant details on animals and/or animal-derived materials used in the study.

Progeria LmnaG609G/G609G mouse model (Lmna tm1.10tin) was used in a C57BL/6N background. Both males and females were used for the study. Samples from wild-type and LmnaG609G/G609G sgRNA-transduced mice were collected at the age of 3.5 months.

Policy information about [studies involving human research participants](#)

12. Description of human research participants

Describe the covariate-relevant population characteristics of the human research participants.

The study did not involve human research participants.